Pharm Res (2015) 32:1128–1140
DOI 10.1007/s11095-014-1524-y

RESEARCH PAPER

Vitamin D Receptor Activation Induces P-Glycoprotein and Increases Brain Efflux of Quinidine:An Intracerebral Microdialysis Study in Conscious Rats

Matthew R. Durk • Jianghong Fan • Huadong Sun • Yingbo Yang • Henrianna Pang • K. Sandy Pang • Inés A. M. de Lannoy

Received: 24 June 2014 / Accepted: 12 September 2014 / Published online: 16 October 2014

ABSTRACT

Purpose Since the vitamin D receptor (VDR) was found to up-regulate cerebral P-glycoprotein expression *in vitro* and in mice, we extend our findings to rats by assessing the effect of rat Vdr activation on brain efflux of quinidine, a P-gp substrate that is eliminated primarily by cytochrome P450 3a.

Methods We treated rats with vehicle or the active VDR ligand, 1α,25-dihydroxyvitamin D_3 [1,25$(OH)_2D_3$] (4.8 or 6.4 nmol/kg *i.p.* every 2nd day ×4) and examined P-gp expression and cerebral quinidine disposition via microdialysis in control and treatment studies conducted longitudinally in the same rat.

Results The 6.4 nmol/kg 1,25$(OH)_2D_3$ dose increased cerebral P-gp expression 1.75-fold whereas hepatic Cyp3a remained unchanged. Although there was no change in systemic clearance elicited by 1,25$(OH)_2D_3$, brain extracellular fluid quinidine concentrations were lower in treated rats. We noted that insertion of indwelling catheters increased plasma protein binding of quinidine and serial sampling decreased the blood:plasma concentration ratio, factors that alter distribution ratios in microdialysis studies. After appropriate correction, $K_{ECF/P,uu}$ and $K_{ECF/B,uu}$, or ratios of quinidine unbound concentrations in brain extracellular fluid to plasma or blood at steady-state, were more than halved.

Conclusion We demonstrate that VDR activation increases cerebral P-gp expression and delimits brain penetration of P-gp substrates.

KEY WORDS blood–brain barrier · microdialysis · P-glycoprotein · vitamin D receptor

ABBREVIATIONS

1,25$(OH)_2D_3$	1α,25-dihydroxyvitamin D_3
aCSF	Artificial cerebrospinal fluid
BBB	Blood–brain barrier
Bcrp/BCRP	Rodent/human breast cancer resistance protein
CAR	Constitutive androstane receptor
CNS	Central nervous system
Cyp	Rodent cytochrome P450
ECF	Extracellular fluid
Gapdh	Glyceraldehyde 3-phosphate dehydrogenase
GR	Glucocorticoid receptor
Mdr1/MDR1	Rodent/human multidrug resistance protein 1
Mrp/MRP	Rodent/human multidrug resistance-associated protein
NR	Nuclear receptors
PBS	Phosphate-buffered saline
P-gp	P-glycoprotein
PMSF	Phenylmethylsulfonyl fluoride
PXR	Pregnane X receptor
qPCR	Quantitative real-time polymerase chain reaction
SDS-PAGE	Sodium dodecyl sulfate polyacrylamide gel electrophoresis
Vdr/VDR	Rodent/human vitamin D receptor

INTRODUCTION

The ability of drugs to cross the blood–brain barrier (BBB) is of critical importance in the development of therapeutics targeting the central nervous system (CNS). The BBB is comprised of endothelial cells surrounding the microvessels that supply nutrients to the brain and glial cells (astrocytes,

MRD and JF contributed equally as first authors and K. Sandy Pang and Inés A.M. de Lannoy are equal co-senior authors

M. R. Durk • K. S. Pang (✉)
Department of Pharmaceutical Sciences, Leslie Dan Faculty of Pharmacy, University of Toronto, 144 College Street, Toronto, Ontario M5S 3M2, Canada
e-mail: ks.pang@utoronto.ca

J. Fan • H. Sun • Y. Yang • H. Pang • I. A. M. de Lannoy
NoAb BioDiscoveries, Mississauga, Ontario, Canada

J. Fan • I. A. M. de Lannoy
InterVivo Solutions, Toronto, Ontario, Canada

microglia and pericytes), working in tandem in what is known as the neurovascular unit [1]. Molecules enter the brain via transcellular diffusion or via influx transporters, which are expressed in endothelial cells. Due to the presence of this glial support network, BBB endothelial cells differ from peripheral endothelial cells in that the tight junctions existing in between them form a barrier and prevent paracellular transport. Moreover, the presence of a multitude of ATP-binding cassette efflux transporters [2], including the multidrug resistance protein 1 (MDR1/P-gp), the multidrug resistance associated proteins (MRP1, MRP3, MRP4, MRP5, and MRP6), and the breast cancer resistance protein (BCRP), is another major deterrent in limiting the entry of drugs to the brain.

The expression of drug transporters at the BBB is under the control of nuclear receptors (NR), notably, the constitutive androstane receptor (CAR) [3], the pregnane X receptor (PXR) [4], the glucocorticoid receptor (GR) [5], and the vitamin D receptor (VDR) [6,7]. PXR and CAR are xenobiotic receptors that respond to exogenous ligands, whereas the GR and VDR respond to endogenous ligands, specifically to glucocorticoids and vitamin D analogs, respectively [8]. The VDR has received considerably less attention than other NRs with respect to the regulation of drug transporters, particularly at the BBB, perhaps because of it being present at very low levels in brain. Only a handful of studies have reported on Vdr/VDR distribution in rat [9] and human [10] brain and examined the role of the VDR in regulating transporters in brain endothelial cells. Treatment with the active VDR ligand, 1α,25-dihydroxyvitamin D_3 [$1,25(OH)_2D_3$] increased P-gp expression and reduced the accumulation of P-gp substrates in Caco-2 cells [11] and brain microvessel endothelial cells [7]. *In vivo* results were in agreement; mice treated with $1,25(OH)_2D_3$ exhibited higher brain P-gp expression and decreased cerebral accumulation of the P-gp substrate, digoxin [6].

The current study extends these findings, using intracerebral microdialysis in a longitudinal study following vehicle-then $1,25(OH)_2D_3$-treatment in the same freely-moving, conscious rat *in vivo*. Beginning as a tool to study changes in neurotransmitter concentrations in time-averaged intervals following administration of a stimulus, the technique of microdialysis has evolved into a means of measuring unbound concentrations of systemically administered drugs in brain extracellular fluid (ECF) over time to assess brain penetration and BBB transport mechanisms [12]. The method is able to directly appraise the blood-to-brain clearance of the P-gp substrate, quinidine, a compound whose clearance in the rat is primarily mediated by hepatic Cyp3a [13] and not by renal P-gp [14]. As a result, changes in P-gp expression are expected to affect the distributional characteristics of quinidine in brain and tissues but not total body clearance. Thus, we chose quinidine to examine the changes in brain distribution in response to $1,25(OH)_2D_3$ treatment. Effects of the activation of rat Vdr on quinidine metabolism and P-gp hepatic and renal expression and changes in unbound plasma or blood fraction and blood to plasma concentration ratio (C_B/C_P) due to catheterization were also investigated. Changes in the unbound brain ECF to unbound plasma/blood concentration ratio at steady-state ($K_{ECF/P,uu}$ or $K_{ECF/B,uu}$) were used to assess the brain distribution due to changes in cerebral P-gp expression. We confirmed that the Vdr expressed in rat brain was activated by $1,25(OH)_2D_3$ though $1,25(OH)_2D_3$ failed to affect liver Cyp3a expression. There was no change in total or unbound quinidine plasma/blood clearances, though the plasma unbound fraction and the blood:plasma concentration ratios were reduced due to catheterization and blood sampling, respectively. Activation of Vdr increased Mdr1/P-gp expression in the rat brain, and decreased $K_{ECF/P,uu}$ and $K_{ECF/B,uu}$, indicative of a net increase in the brain-to-blood clearance of the P-gp substrate, quinidine.

MATERIALS AND METHODS

Reagents and Materials

$1,25(OH)_2D_3$ (Fluka AG) and quinidine were purchased from Sigma Aldrich Canada (Mississauga, ON), whereas deuterated quinidine (d3-quinidine) was obtained from Toronto Research Chemicals (Toronto, ON); lidocaine was a kind gift from AB Sciex (Concord, ON). All reagents for quantitative real-time polymerase chain reaction (qPCR) were obtained through Life Technologies (Foster City, CA). The C219 primary antibody for immunoblotting and immunostaining of P-gp was purchased from ID Labs (London, ON). The Vdr (9A7), Bcrp (BXP53) and glyceraldehyde-6-phosphatase (Gapdh) primary antibodies (6C5) were from Abcam (Cambridge, MA); the primary antibody to Mrp1 was obtained from Kamiya Biomedical (Seattle, WA) and the Mrp4 primary antibody was a kind gift of Dr. John Schuetz, St. Jude Children's Research Hospital (Memphis, TN). Secondary antibodies for immunoblotting were obtained from BioRad (Mississauga, ON) and secondary fluorescent antibodies for immunostaining: Alexa Fluor 488 (FitC) goat anti-mouse (A11001) and Alexa Fluor 546 (TritC) goat anti-rat (A11081) were from Molecular Probes (Invitrogen, Burlington, ON). The equipment used for microdialysis was purchased from BASi (West Lafayette, IN), including tubing used for probes and IV infusion, whereas microdialysis probes (CMA12 - 3 mm) were obtained from CMA Microdialysis AB (Holliston, MA).

Rats

Male Sprague Dawley rats weighing 300–325 g were obtained from Charles River (St. Constant, QC) and maintained on a

12 h light - dark cycle with access to food and water *ad libitum*. Rats used for microdialysis, protein binding and blood:plasma concentration ratio studies were housed in the animal facility at NoAb BioDiscoveries and InterVivo Solutions, respectively; all procedures were reviewed by the corresponding Institutional Animal Care Committees and carried out in accordance with guidelines of the Canadian Council on Animal Care. Rats used for other studies were housed in the animal facility at the University of Toronto, and protocols for these studies were approved by the University of Toronto Animal Care Committee. Rats received an intraperitoneal (*i.p.*) dose of 0, 4.8 or 6.4 nmol/kg of $1,25(OH)_2D_3$ in filtered, sterile corn oil (1 ml/kg). For the collection of tissues 2 days after the final dose, rats were anesthetized with ketamine/xylazine and exsanguinated by transcardial perfusion with cold saline. Brains were snap-frozen in liquid nitrogen and stored at −80°C until analysis. For mRNA and protein analyses, n= 3–4 per group; for microdialysis studies, n=6; for protein binding studies, n=7–9 for each plasma collection time point.

Immunostaining

Immunostaining was carried out on sections cut from paraffin-embedded tissues. Briefly, rats were anesthetized by ketamine/xylazine and perfused transcardially with phosphate-buffered saline (PBS) and then with 4% paraformaldehyde in PBS. Brain tissues were post-fixed overnight in 4% paraformaldehyde, processed and embedded. Sections of 7 microns in thickness were cut using a microtome and mounted onto slides, which were pre-coated in poly-L-lysine. Mounted sections were dried overnight, dewaxed then underwent antigen retrieval, which entailed incubation in 10 mM sodium citrate, pH 6.0, followed by incubation in 2 N HCl at 37°C for 30 min. Sections were pre-blocked in 5% goat serum in PBS containing 0.1% Tween 20, which were then incubated with primary antibodies to P-gp and Vdr overnight at a dilution of 1:50 v/v in pre-block solution. Sections were rinsed 3x with pre-block solution and incubated with fluorescent secondary antibodies for 2 h at room temperature, then washed and imaged using a Nikon E1000R fluorescence microscope. The specificity of the C219 antibody and 9A7 antibody staining was verified in brains of *mdr1a/b*$^{-/-}$ (Taconic Farms, Germantown, New York) and *vdr*$^{-/-}$ (B6.129S4-Vdr^{tm1Mbd}/J) (Jackson Laboratories, Bar Harbor, Maine) mice, respectively (data not shown).

Protein Binding

Since catheterization over an extended period of time may alter the plasma protein binding of drugs due to an increase in serum albumin or α_1-acid glycoprotein [15] and influence the binding, distribution and elimination of quinidine [14], plasma protein binding was studied during the time course of the experiment. Using equilibrium dialysis, we determined the extent of quinidine plasma protein binding (unbound fraction in plasma, $f_{u,P}$) in rats with indwelling venous and arterial catheters implanted for 12 and 22 days, the times for the microdialysis studies in control and $1,25(OH)_2D_3$ treated rats, respectively. We compared $f_{u,P}$ values of day 12 and day 22 with those of the uncatheterized rat. To determine $f_{u,P}$, we used a high-throughput dialysis apparatus (Model HTD96b, HTDialysis, Gales Ferry CT) according to the manufacturer's protocol. Briefly, 150 µl plasma sample containing quinidine, present at a final concentration of 250 ng/ml, was added to the donor compartment and equilibrated against 150 µl blank PBS buffer in the receiver compartment at 37°C for 16 h, during which time the dialysis apparatus was maintained on a shaking incubator. Thereafter, 50 µl of plasma and 100 µl of PBS were removed from each donor and receiver compartment, respectively, and diluted with 100 µl blank PBS or 50 µl of blank plasma. Quinidine concentration in each sample was quantified by LC-MS/MS, as described below. These measured $f_{u,P}$ values were then used to appraise the unbound quinidine clearances for the control- and $1,25(OH)_2D_3$-treatment periods, respectively.

Determination of Blood: Plasma Concentration Ratio (C_B/C_P)

The blood-plasma distribution of quinidine was examined before and after implantation of the indwelling catheters. On day 0, catheters were implanted in one set of rats, and on day 12 after implantation, blood samples (100 µl) were taken at the same time points used for microdialysis studies (45, 75, 105, 135, 195, 255, 315, 345, 375, 405, 435, 465 and 495 min). The last 7 samples were pooled, aliquotted and spiked with various concentrations of quinidine (to final concentrations of 10, 50, 100, 300, 500 and 800 ng/ml), and allowed to equilibrate for 30 min in a shaking incubator at 37°C. Following incubation, blood (25 µl) was removed for analysis and other aliquots were used for the determination of the hematocrit (HCT) and to provide plasma. The procedure was repeated on day 22. From the blood: plasma concentration (C_B/C_P) ratio, we estimated the fraction unbound in blood ($f_{u,B}$) for each group using Eq. 1 and the unbound fraction in red blood cells ($f_{u,RBC}$) using Eq. 2 [16].

$$f_{u,B} = \frac{f_{u,P}}{C_B/C_P} \tag{1}$$

$$f_{u,RBC} = \frac{HCT}{\frac{1}{f_{u,B}} - \frac{1-HCT}{f_{u,P}}} \tag{2}$$

Microsomal Metabolism

To ascertain whether $1,25(OH)_2D_3$ treatment altered hepatic metabolism, we compared quinidine decay rate constants in liver microsomal preparations from control and treated rat livers (0 or 6.4 nmol/kg q2d *i.p.* × 4). Briefly, liver tissue was dounce homogenized in 4× (w/v) buffer (1.15% KCl, 20 mM Tris–HCl, pH 7.4) and centrifuged at 9,000 × *g* for 20 min at 4°C. The resulting supernatant was centrifuged at 100,000 × *g* for 60 min at 4°C and the pellet was re-suspended. Following protein quantification by the Lowry assay, 10 μM quinidine was incubated with 0.2 mg of microsomal protein in 200 μl of buffer containing 100 mM Na_2HPO_4, pH 7.4, with an NADPH-generating system (BD Biosciences, Woburn, MA) at a final concentration of 1.55 mM $NADP^+$, 3.3 mM glucose-6-phosphate, 3.3 mM $MgCl_2$, 0.4 U/ml glucose-6 phosphatase and 0.05 mM sodium citrate at 37°C, according to the manufacturer's protocol. Negative controls, either with microsomal protein denatured by heat inactivation prior to incubation or with NADPH absent from the incubation mixture, were included. At various time-points, the reaction was terminated by addition of 200 μl ACN to the incubation mixture. Samples were assayed by LC-MS/MS (see below).

Estimation of Microdialysis Recovery of Quinidine *in Vitro* and *in Vivo*

A major limitation of the microdialysis method is an accurate estimation of recovery of analyte in the system, since the concentration measured in the dialysate does not reflect the true concentration in the brain ECF [17]. Microdialysis probes (CMA 12, CMA Microdialysis AB) were placed in 1.5 ml tubes (reservoirs) containing artificial CSF (aCSF, 147 mM NaCl, 2.7 mM KCl, 1.2 mM $CaCl_2$, 0.85 mM $MgCl_2$) and were perfused at 0.5 μl/min for 4 h via a pump (Harvard Apparatus, Holliston, MA). Dialysate was collected with a fraction collector (BASi, West Lafayette, IN). In the first *in vitro* study, perfusate containing 100 ng/ml quinidine and a 1.5 ml reservoir containing 100 ng/ml d3-quinidine were used to measure R_{loss} $[1\text{-}(C_{dialysate\text{-}d0}/C_{perfusate\text{-}d0})]$ for quinidine, and R_{gain} $(C_{dialysate\text{-}d3}/C_{reservoir\text{-}d3})$ for d3-quinidine. In the second *in vitro* study, placement of quinidine in the perfusate and d3-quinidine in the reservoir was reversed. No difference was observed between R_{loss} and R_{gain} for both quinidine and d3-quinidine (Table I). With use of d3-quinidine together with quinidine, we were able to determine the recovery of quinidine, and were the first to employ the *in vitro* loss/gain method to verify that recovery by loss (R_{loss}) equalled the recovery by gain (R_{gain}) [18]. After confirmation of the recovery from the *in vitro* experiments, we proceeded to estimate recovery *in vivo* by retrodialysis, calculating the d3-quinidine loss from perfusate $[1\text{-}(C_{dialysate,d3}/C_{perfusate,d3})]$ during the microdialysis experiment. This value was assumed to equal the recovery by gain $(C_{dialysate,d0}/C_{u,ECF,d0})$ at each time-point. The relation was used to estimate $C_{u,ECF}$ values (for diagram, see Fig. 4a). The study was carried out three times.

Table I *In vitro* recoveries (R), by Loss and Gain of Quinidine and d3-Quinidine. Data Represent the Mean ± S.E.M. ($n = 3$)

	R_{loss}	R_{gain}
Quinidine	0.576 ± 0.0508	0.530 ± 0.0717
d3-Quinidine	0.591 ± 0.0514	0.501 ± 0.0451

Surgical Procedures for Microdialysis Studies

On day 0, venous and arterial catheters and two microdialysis guide cannulae, one in the striatum of each (left and right) hemisphere of the brain, were implanted into the rat under isofluorane anesthesia. One catheter (CX-2021S, BASi) was inserted into the femoral vein and another catheter (CX-8002S, BASi) was inserted into the femoral artery of the same leg and then both were secured into place. The catheters were exteriorized through a small incision made at the nape of the neck. On the same day, guide cannulae were implanted in the striatum (AP 0.2, ML±2.8, DV±3.6); the anesthetized rat was placed in a stereotaxic instrument, and a 2 cm lateral incision was made to expose the skull. Two small holes were drilled through the skull [AP 0.2 mm, ML±2.8 mm relative to bregma] and then two guide cannulae containing dummy probes were gently lowered into the skull (3.6 mm DV) using the stereotaxic instrument and anchored into place with dental cement (GC FujiCEM AutoMix, Tokyo, Japan) via anchor screws. The incision was sutured, after which a small dose of antibiotic (penicillin, 6000 IU/kg) was injected subcutaneously along with 2 ml of saline to rehydrate the animal. Catheters were flushed daily with heparinized saline to maintain patency.

Microdialysis Study

Two consecutive microdialysis experiments were carried out in each rat in order to compare the effect of vehicle and $1,25(OH)_2D_3$ treatment on brain quinidine distribution in the same rat, thereby reducing inter-animal variability. Four days after recovery from surgery (day 4), rats received corn oil, given intraperitoneally (*i.p.*) every second day for 8 days. The first microdialysis study with quinidine was conducted 2 days after the final corn oil injection (day 12). In the next phase of the study, the same rat received 6.4 nmol/kg $1,25(OH)_2D_3$ *i.p.* every second day for the next 8 days, after a 2-day wash-out period. The second microdialysis study was conducted 2 days after the final $1,25(OH)_2D_3$ dose (day 22). After completion of the second phase, the rat was sacrificed and terminal blood and tissues were collected for analyses.

For vehicle-treated rats, the probe that was inserted into the right striatum was used for the microdialysis study; for continuation of the study following $1,25(OH)_2D_3$ treatment in the same rat, the probe inserted into the left striatum was used, and each probe was not re-used. We first verified, in separate studies, that no difference existed for the left and right whole brain quinidine concentrations following *i.v.* quinidine infusion for untreated rats (data not shown). One day prior to each microdialysis study, rats were placed in RATURN cages (BASi), and the microdialysis probes were inserted into the appropriate guide cannulae and perfused with artificial aCSF overnight at a rate of 0.1 µl/min to equilibrate and allow for the removal of substances in the ECF that may have been released as a result of the insertion of the probe. One h before the study, the flow rate was increased to 0.5 µl/min, and the aCSF was switched to aCSF-containing d3-quinidine solution (100 ng/ml). At the start of study, an intravenous bolus dose of 6 mg/kg quinidine (loading dose), dissolved in 0.9% NaCl containing 10% ethanol, was administered into the femoral vein catheter, and infusion was initiated immediately thereafter, with 27.91 µg/min/kg of quinidine delivered at 1.9 µl/min. Dialysate from the microdialysis probe was collected at 30 min intervals for 480 min by the fraction collector into refrigerated tubes. About 100 µl of blood was removed from the femoral artery catheter into a heparinized tube at the midpoint of each dialysate collection interval (T_{mid}) to provide plasma obtained upon centrifugation (3200 × *g* for 5 min at 4°C).

Quantification of Quinidine by LC-MS/MS

Analysis of quinidine and d3-quinidine was performed by an API4000 and API4000 QTRAP liquid chromatography/mass spectrometric system (LC-MS/MS, AB Sciex, Concord, ON), including an Agilent 1100 liquid chromatograph with degasser, binary pump, HTC-PAL autosampler (Leap Technologies, Carrbiri, NC) and a mixer (Upchurch). Chromatographic separation of analytes and internal standard (IS) was performed utilizing a Zorbax XDB-C18 column (2.1 × 30 mm, VWR, Mississauga, ON) and liquid gradient chromatography, using an assay developed and qualified by NoAb BioDiscoveries. Mobile phase A (MP-A) consisted of 10 mM ammonium formate, pH 3.0, and mobile phase B (MP-B) consisted of methanol/10 mM ammonium formate (pH 3.0) (95/5, v/v). Ten percent of MP-B was delivered for 0.4 min, and then increased to 40% at 0.5 min and maintained until 1.1 min, increased to 95% at 1.2 min where it remained until 1.7 min, then returned back to 10% at 1.8 min for 0.2 min. Analytes were determined in positive ion electrospray mode using selected reaction monitoring (SRM or MRM) and the peak area of analyte was divided by that of the internal standard (IS), lidocaine. The ion transitions (m/z) that were monitored were 325.2/172.1/79.0, 328.2/79.1/175 and 235.1/86.0 for quinidine, d3-quinidine and lidocaine, respectively. Calibration standards, prepared by spiking the appropriate analytes and IS in each blank matrix (inactivated microsomes, PBS, blood, plasma, brain homogenate and aCSF), were utilized for quantification.

Brains, taken after completion of the second microdialysis study, were homogenized in 2x (w/v) of phosphate-buffered saline. An aliquot (100 µl) of 50:50 methanol/acetonitrile containing the IS was added to an aliquot of plasma (10 µl), blood (10 µl) or brain homogenate (20 µl) sample or calibration standard for the precipitation of proteins. After centrifugation at 12,000 rpm and 4°C for 5 min, the supernatant was either dried down under a gentle stream of N_2, then reconstituted with MP-A, or diluted with MP-A. An aliquot (20 µl) was then injected into the LC-MS/MS system. For dialysate samples and aCSF calibration standards, 5 µl was diluted in 30 µl of mobile phase containing IS, and 20 µl was injected.

Assessing BBB Permeability

The unbound fraction of quinidine in rat brain homogenate ($f_{u,Br}$) was previously determined by equilibrium dialysis to be 0.0807 (NoAb BioDiscoveries, unpublished data). With this known value of $f_{u,Br}$ and the estimated $f_{u,P}$, we were able to calculate the unbound brain concentration ($C_{u.Br,ss}$) and the unbound concentration in plasma ($C_{u,P,ss}$) at steady-state, and subsequently assess the intra-brain distribution by comparing the K_P values and the unbound distribution volume of drug in brain ($V_{u,Br}$) determined from the total amount in brain at steady-state ($A_{Br,ss}$) according to the formulae shown below:

$$K_{Br/P} = \frac{C_{Br,ss}}{C_{P,ss}} \tag{3}$$

$$K_{Br/P,uu} = \frac{C_{u,Br,ss}}{C_{u,P,ss}} \tag{4}$$

$$K_{ECF/P,uu} = \frac{C_{u,ECF,ss}}{C_{u,P,ss}} \; and \; K_{ECF/B,uu} = \frac{C_{u,ECF,ss}}{C_{u,B,ss}} \tag{5}$$

$$V_{u,Br} = \frac{A_{Br,ss}}{C_{u,ECF,ss}} \tag{6}$$

Values of $K_{ECF/P,uu}$ and $K_{ECF/B,uu}$ were compared between vehicle and $1,25(OH)_2D_3$-treated rats.

Real-Time PCR

Total mRNA was extracted using TRIzol according to the manufacturer's protocol. cDNA was constructed using a high capacity cDNA kit (Life Technologies), and qPCR was carried out using an Applied Biosystems 7500 Real-Time PCR system, as previously described [7]. Table II lists the primers used for qPCR.

Immunoblotting

Immunoblotting was conducted as previously described in detail [7]. Briefly, tissue was homogenized to provide a crude membrane fraction, and protein concentration was determined by the Lowry assay [19]. Aliquots containing 50 μg protein were resolved on SDS-PAGE gels and transferred to a nitrocellulose membrane. Membranes were blocked in 5% skim milk for 1 h and incubated with primary antibodies overnight. Following incubation with secondary antibody for 2 h, bands were visualized with enhanced chemiluminesence reagent (GE Healthcare, Pittsburgh, PA) and quantified by densitometry (Scion Image, National Institutes of Health). Proteins of similar molecular weights were resolved on different gels and normalized to their respective Gapdh bands.

Statistical Analyses

Differences between vehicle- and $1,25(OH)_2D_3$–treated rats were assessed using Student's two-tailed t test if comparing only two groups. When comparing more than 2 groups, ANOVA, followed by Bonferroni's multiple comparisons test was used. For the microdialysis studies, a paired two-tailed t test was used. Results with a p value of less than 0.05 were considered to be significantly different.

RESULTS

P-gp and Vdr Are Co-Expressed in Rat Brain Capillary Endothelia

Immunohistochemistry studies in rat brain (Fig. 1) showed that P-gp was present in the capillary endothelial cell membrane and that Vdr was present within nuclei of endothelial cells. Weak Vdr staining was also observed in nuclei of the surrounding neurons. The specificity of the P-gp antibody was verified by the lack of staining observed in tissue of an *mdr1a/b*(−/−) mouse (not shown), and additionally, staining for Vdr in a $vdr^{(-/-)}$ mouse did not elicit a signal in brain or kidney sections (not shown). When sections were incubated with secondary antibody only, no staining was observed (not shown).

$1,25(OH)_2D_3$ Treatment Induces Rat Brain Cyp24a1 and Mdr1a mRNA and P-gp Protein Expression

Expression of Cyp24a1, a VDR target gene that is responsible for the metabolism of $1,25(OH)_2D_3$ [20], was used as a marker of Vdr activation. Indeed, treatment of rats with $1,25(OH)_2D_3$ increased brain Cyp24a1 mRNA expression in a dose-dependent manner, ranging from 2.25-fold (non-significant) for the low dose to 4.5-fold ($p<0.05$) for the higher dose. The higher dose also led to higher (50%) Mdr1a mRNA expression (Fig. 2a) and increased P-gp protein levels by 70% (Fig. 2b). An inductive trend was also seen for the lower dose, though the changes were not statistically significant. Mrp1 mRNA levels were slightly lowered with the 4.8 nmol/kg but not the 6.4 nmol/kg dosing regimen (Fig. 2a), and there was no change in Mrp1 protein (Fig. 2b). Mrp4, Bcrp and VDR mRNA and protein levels were unchanged following the $1,25(OH)_2D_3$ treatment doses (Figs. 2a and 2b).

Table II Primers Used for qPCR

Gene	GenBank number	Forward (5′→3′ Sequence)	Reverse (5′→3′ Sequence)
Gapdh	NM_017008	TGAAGGTCGGTGTGAACGGATTTGGC	CATGTAGGCCATGAGGTCCACCAC
Vdr	NM_017058	ACAGTCTGAGGCCCAAGCTA	TCCCTGAAGTCAGCGTAGGT
Cyp24a1	NM_201635	GCATGGATGAGCTGTGCGA	AATGGTGTCCCAAGCCAGC
Mdr1a	NM_133401	GGAGGCTTGCAACCAGCATTC	CTGTTCTGCCGCTGGATTTC
Mdr1b	NM_012623	GGACAGAAACAGAGGATCGC	TCAGAGGCACCAGTGTCACT
Mrp1	NM_022281	AGAAGGAATGTGTTAAGTCGAGGAA	CCTTAGGCTTGGTGGGATCTT
Mrp4	NM_133411	GCCCTTACCCAGCTGCTGA	CAGAATCCAGAGAGCCTCTTTTACA
Bcrp	NM_181381	ATGATGCTCTTTTCTGGCCTCT	AAGCCATATCGAGGAATGCTAAA

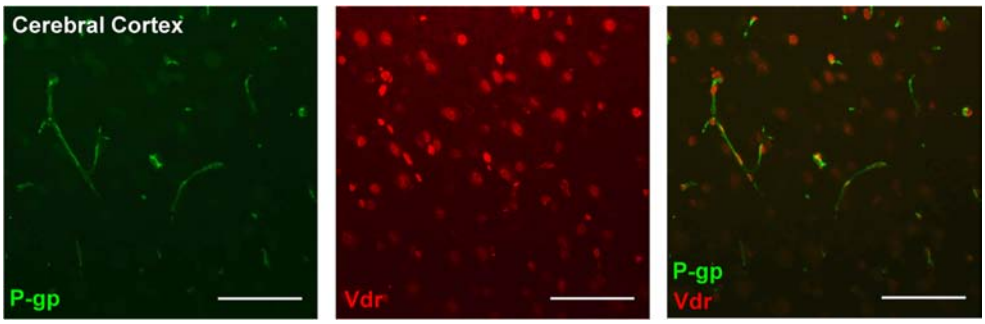

Fig. 1 Immunostaining for P-gp (*green*) and Vdr (*red*) in the rat cerebral cortex. In the cerebral cortex, P-gp staining was seen in cortical capillaries, while Vdr staining was mostly nuclear, and observed in both capillaries and cortical neurons.

Plasma Protein Binding and Blood Distribution Following Indwelling Catheter Implantation

Changes in protein binding of quinidine, pre- and post-surgery, are summarized in Table III. The value of $f_{u,P}$ for quinidine in plasma obtained from rats pre-surgery was 0.364 ± 0.0156. The value of $f_{u,P}$ was decreased significantly ($p < .05$) to 0.238 ± 0.0363 on day 12 after catheterization of the femoral vein and artery, the time for the vehicle-treatment microdialysis study. The value of $f_{u,P}$ rose slightly back to 0.300 ± 0.0241 on day 22, the time for the second microdialysis study following $1,25(OH)_2D_3$-treatment; the value was not statistically different compared to that on day 12. From these values, we were able to estimate the fraction of quinidine unbound in blood and red blood cells (Table III). These two $f_{u,P}$ values were used to determine the unbound plasma concentrations in vehicle- and $1,25(OH)_2D_3$-treated rats, respectively. There were also changes in the C_B/C_P concentration ratio, pre- and post-implantation (Table IV). The C_B/C_P value was, on average, about 1.4 pre-surgery, but decreased to 0.83 for both day 12 and day 22 post-catheterization. As shown, these are consequences of changes in plasma protein binding and a decline in the hematocrit, likely due to continuous sampling. These values were used in the estimation of plasma and blood clearances, summarized in Table V.

$1,25(OH)_2D_3$ Treatment and Liver Cyp3a and Liver and Renal P-gp Levels

Since quinidine is eliminated almost exclusively by hepatic Cyp3a in the rat, with only 2% of quinidine excreted unchanged into urine [14], possible changes in Cyp3a protein expression and function in liver tissue with $1,25(OH)_2D_3$ treatment were examined. No change was found in Cyp3a protein expression (Fig. 3a) or in rates of quinidine metabolism in microsomal incubations (1 mg/ml protein) prepared from livers of vehicle- *versus* $1,25(OH)_2D_3$-treated rats. Because of >15% depletion of substrate, the disappearance rate constant of quinidine was evaluated from the log linear decay of quinidine concentration *vs.* time plot. No difference in the first-

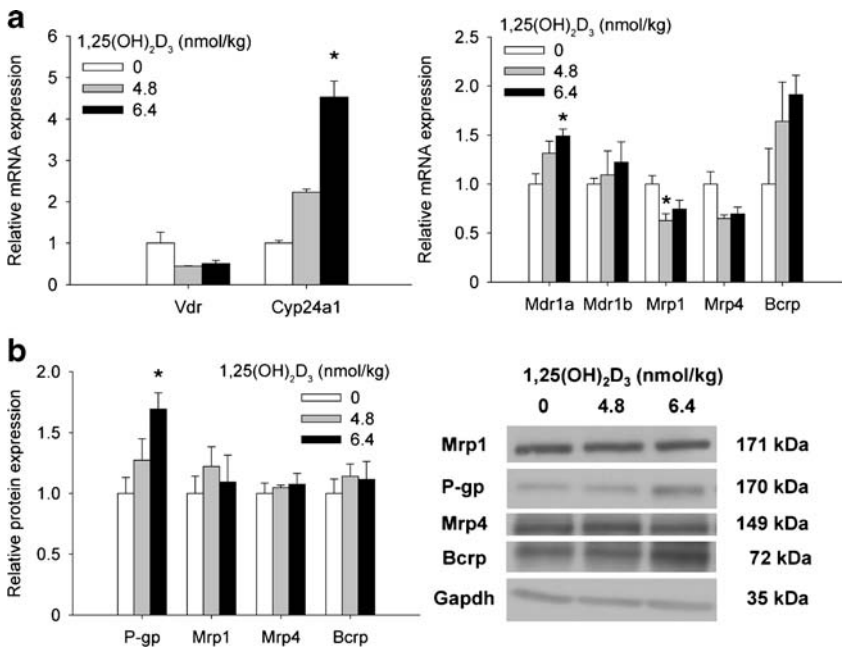

Fig. 2 Changes in mRNA of Vdr target genes and transporters (a) and protein expression of transporters (b) in the rat whole brain following treatment with 0, 4.8 or 6.4 nmol/kg $1,25(OH)_2D_3$, q2d × 4. Treatment with $1,25(OH)_2D_3$ induced Cyp24a1 in a dose-dependent manner, and the higher dose elicited an increase in Mdr1a mRNA and P-gp protein. Data are presented as mean ± S.E.M. "*" denotes $p < 0.05$ according to one-way ANOVA and Bonferroni's multiple comparisons test.

Table III Catheterization of the Femoral Artery and Femoral Vein Alters Hematocrit and Protein Binding of Quinidine in Plasma, Whole Blood and Red Blood Cells. Data Represent the Mean ± S.E.M. ($n \geq 6$ for each group)

	HCT	$f_{u,P}$	$f_{u,B}$[a]	$f_{u,RBC}$[b]
Pre-surgery	0.419 ± 0.00427	0.364 ± 0.0152	0.249 ± 0.0104	0.182 ± 0.00758
Day 12 (control study)	0.344 ± 0.0142*	0.238 ± 0.0363*	0.286 ± 0.0437	0.377 ± 0.0575*
Day 22 (treatment study)	0.361 ± 0.0055*	0.300 ± 0.0241	0.361 ± 0.0291*	0.476 ± 0.0383*

* denotes $p < 0.05$ between pre-surgery and post-catheter implantation according to 1-way ANOVA and Bonferonni's multiple comparisons test

[a] estimated from Eq. 1, averaged values in Table IV

[b] estimated from Eq.2

order elimination rate constant (k), based on total quinidine decay, was found between vehicle-treated *vs.* $1,25(OH)_2D_3$-treated preparations (Fig. 3b), an observation expected due to the low level of Vdr in the rat liver [21]. The apparent intrinsic clearances (k x volume of incubation mixture) were 0.0318 ± 0.00672 and 0.0289 ± 0.0128 ml/min/mg protein, respectively. In view of the lack of change, it may be concluded that the hepatic intrinsic clearance for quinidine metabolism also remained unchanged. In accompanying liver and kidney tissues, a two-fold induction in hepatic (Fig. 3a) and renal P-gp expression (Fig. 3c) was observed.

$1,25(OH)_2D_3$ Treatment Alters Distribution of Quinidine in Rat Brain ECF But Not Systemic Clearance

Immediately after the intravenous bolus dosing and commencement of intravenous infusion, unbound plasma quinidine concentrations reached steady-state as early as the first sampling time-point, and were virtually identical for both control and treated rats (Fig. 4b). These were 79.0 ± 10.8 ng/ml for vehicle-treatment and 116 ± 1.9 ng/ml for $1,25(OH)_2D_3$-treatment, respectively ($p > .05$), yielding similar plasma clearances of 99.6 and 89.8 ml/min/kg. Both the plasma clearance and pre-surgical C_B/C_P values agreed well with published quinidine pharmacokinetics data in the rat [22]. With a C_B/C_P ratio of 0.83, blood quinidine clearances were found to be similar at 120 and 108 ml/min/kg, respectively (Table V). These values are similar to that of liver blood flow [23].

Brain ECF quinidine concentrations (dialysate concentrations, corrected for *in vivo* recovery of the microdialysis system) peaked immediately following the loading dose and decreased gradually for 3 h, after which levels remained relatively stable. The steady-state brain ECF quinidine concentrations were significantly lower in $1,25(OH)_2D_3$-treated rats (12.5 ± 1.47 ng/ml), being about half of those observed for control rats (25.3 ± 5.34 ng/ml) (Fig. 4b). A significantly lower (2.5-fold) steady-state unbound brain ECF: plasma concentration ratio ($K_{ECF/P,uu}$) for quinidine resulted with treatment (0.123 ± 0.0223 *vs.* 0.324 ± 0.0398) (Fig. 4b); a similar change in $K_{ECF/B,uu}$ values was observed. Changes in these parameters between control and $1,25(OH)_2D_3$-treated rats are summarized in Table V. Brain P-gp levels at sacrifice (22 days) showed on average, a 55% increase in cerebral P-gp expression (Fig. 4c) for $1,25(OH)_2D_3$-treated *vs.* control rats, suggesting that increasing expression of the efflux transporter had increased quinidine efflux at the BBB.

Table IV Catheterization of the Femoral Artery and Femoral Vein Alters the Quinidine Blood: Plasma Concentration Ratios. Data Represent the Mean ± S.E.M. ($n = 4$ for Each Group)

Blood concentration (ng/ml)	C_B/C_P Ratio		
	Pre-surgery	Day 12 (control study)	Day 22 (treatment study)
10	1.36 ± 0.0435	0.815 ± 0.0639*	0.756 ± 0.0579*
50	1.42 ± 0.101	0.839 ± 0.0732*	0.797 ± 0.0427*
100	1.55 ± 0.0601	0.857 ± 0.0387*	0.857 ± 0.0529*
300	1.41 ± 0.0844	0.854 ± 0.0412*	0.843 ± 0.0182*
500	1.48 ± 0.0522	0.822 ± 0.0698*	0.877 ± 0.0235*
800	1.57 ± 0.0242	0.812 ± 0.0746*	0.863 ± 0.0728*

* denotes $p < 0.05$ between pre-surgery and post-catheter implantation according to 2-way ANOVA and Bonferonni's multiple comparisons test.

Table V Pharmacokinetics of Quinidine after Intravenous Infusion to Control *vs.* 1,25(OH)$_2$D$_3$-Treated Rats Undergoing Microdialysis in the Longitudinal Study (Values are Mean ± S.E.M., $n = 6$)

Parameters	1,25(OH)$_2$D$_3$ (nmol/kg*i.p.*, q2d × 4)	
	0	6.4
Microdialysis recovery at ss *in vivo*	0.355 ± 0.0280	0.396 ± 0.0657
Infusion rate k_0 (μg/min/kg)	27.9	27.9
$f_{u,P}$	0.238 ± 0.0363	0.300 ± 0.0241
C_B/C_P	0.833 ± 0.00805	0.832 ± 0.0190
$C_{P,\ ss}$ (ng/ml)	333 ± 45.4	386 ± 73.0
$C_{B,ss}$ (ng/ml)	277 ± 37.7	321 ± 60.6
$C_{u,Pss}$ (ng/ml)	79.0 ± 10.8	116 ± 21.9
$C_{u.ECF,ss}$ (ng/ml)	25.3 ± 5.34	12.5 ± 1.47*
$C_{u,Br,ss}$ (ng/g)	N/A	6.92 ± 0.445
$V_{u,Br}$ (ml)	N/A	7.19 ± 0.613
$K_{Br/P}$ ($C_{Br,\ ss}/C_{P,\ ss}$)	N/A	0.199 ± 0.02
$K_{Br/P,uu}$ ($C_{u,Br\ ss}/C_{u,P,\ ss}$)	N/A	0.0676 ± 0.0091
$K_{ECF/P,uu}$ ($C_{u,ECF\ ss}/C_{u,P,\ ss}$)	0.324 ± 0.04	0.123 ± 0.022*
$K_{ECF/B,uu}$ ($C_{u,ECF\ ss}/C_{u,B,\ ss}$)	0.390 ± 0.060	0.149 ± 0.027*
CL_P ($k_0/C_{P,\ ss}$) (ml/min/kg)	99.6 ± 15.9	89.8 ± 14.4
CL_B ($k_0/C_{B,\ ss}$) (ml/min/kg)	120 ± 19.2	108 ± 17.4

N/A denotes "not available", since the rat was not sacrificed at day 12 for the first microdialysis study.

"*" denotes $p < 0.05$ between vehicle- and 1,25(OH)$_2$D$_3$-treated rats, according to a paired Student's *t* test

DISCUSSION

The role of the vitamin D receptor in the CNS has received limited attention until recently. While VDR expression and function have been well-characterized in the kidney and intestine, the presence of VDR in brain is less studied, although Vdr/VDR protein has been identified in rodent [9] and human [10] brains. In the rat, we observed that Vdr protein expression is mainly in the nuclei of neurons and capillary endothelia, while observations by Prufer *et al.* [9] described widespread Vdr staining in the rat cerebral cortex and pyramidal neurons of the hippocampus, particularly CA1 and CA3, as well as high immunoreactivity in the Purkinje cells of the cerebellum. In the human brain, results are similar, yet VDR distribution appears to be more widespread than that in rodents [10].

As the presence of VDR in the CNS becomes more recognized, vitamin D deficiency has coincidently been linked to numerous disease states, including Alzheimer's disease [24, 25], Parkinson's disease [26], and epilepsy [27,28]. It has been suggested that vitamin D has many neuroprotective functions, with VDR activation stimulating the release of nerve growth factor [29], suggesting that VDR may be essential for neuron differentiation and the release of glial cell line-derived neurotropic factor [30]. In addition, VDR is involved in the maintenance of Ca^{2+} homeostasis in brain and is critical for proper functioning of neurons. VDR activation lowers L-type voltage-gated Ca^{2+} channel activity by both genomic [31] and non-genomic [32] actions, possibly reducing Ca^{2+}-induced excitotoxicity in neurons.

While numerous studies have concentrated on VDR-mediated Mdr1/P-gp induction in eliminating organs, relatively little work has examined the phenomenon in brain capillary endothelial cells. It was shown that rat and human brain microvessel endothelial cell cultures responded to 1,25(OH)$_2$D$_3$ treatment in a dose-dependent manner. This led to increased P-gp function, measured by the reduction of rhodamine 6G accumulation in endothelial cells, an effect that was negated upon pretreatment with a P-gp inhibitor [7]. While the *in vitro* work demonstrates both the presence and activity of Vdr/VDR in brain capillary endothelia, the present work confirms that similar observations occur *in vivo*. Our study sheds further light on an additional role for the vitamin D receptor in the CNS: regulation of Mdr1/P-gp at the BBB. P-gp possesses a wide substrate specificity, including vinca alkyloids, anthracyclines, epipodophyllotoxins, taxanes, HIV protease inhibitors, as well as some endogenous compounds, including steroids and some peptides [33], such as amyloid-β [34]. Because the CNS is susceptible to relatively small amounts of toxic substances, P-gp acts as a gatekeeper at the BBB; however, for drugs targeting the brain, P-gp induction can also lead to insufficient therapeutic levels in the brain.

In vivo observations on P-gp function may be readily appraised by microdialysis, which allows for serial estimation of unbound drug concentrations in the brain ECF. For most CNS drugs, measuring the unbound ECF concentration is highly pertinent, as it is generally accepted that it is the unbound drug that interacts with its therapeutic target [35]. However, the injury sustained during probe implantation for microdialysis studies may lead to inflammation and neuronal cell death [36] and result in incorrect estimates of BBB permeability for the drug tested. By performing the control and 1,25(OH)$_2$D$_3$ treatment in a longitudinal study, we are able to assess changes in quinidine brain distribution within the same animal, minimizing issues of inter-animal surgical variability that can alter BBB permeability. At the same time, we avoided undertaking more than two microdialysis studies using the same probe on the animal, which has been suggested to alter BBB permeability [37]. By implanting two probes in the initial surgical procedure and avoiding re-using probes between the first and second studies, we minimized variations in drug recovery between control and treatment conditions. By overcoming these limitations, microdialysis emerges as a highly reliable and effective method of assessing transporter-mediated alterations of BBB permeability [38–40]. One drawback, however, remains. Because of the sequential

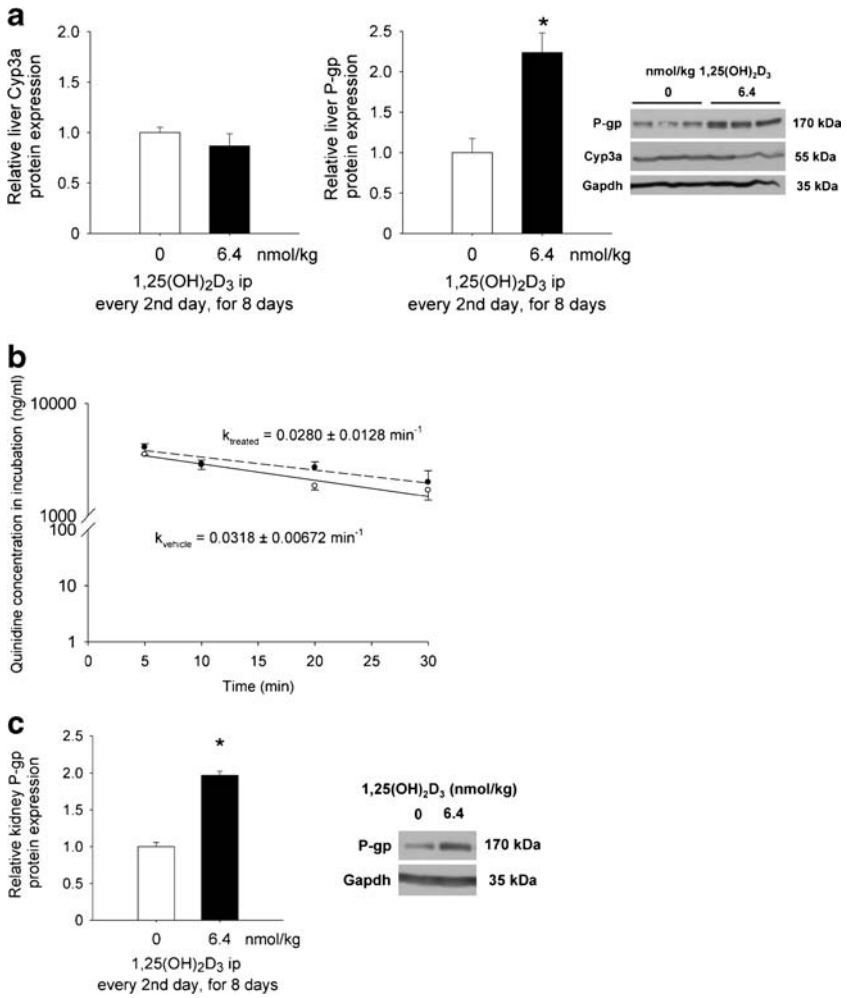

Fig. 3 Changes in hepatic and renal P-gp, and hepatic Cyp3a protein expression and function following 1,25$(OH)_2D_3$ treatment. Hepatic (a) and renal (c) P-gp protein expression were induced whereas hepatic Cyp3a protein expression (a) and function (b) remained unchanged in treated compared to control rats. Data are mean ± S.E.M. "*" denotes $p < 0.05$ according to Student's two-tailed *t* test.

manner of the microdialysis studies, rats were not sacrificed after the control treatment period to determine the unbound brain concentrations (to approximate $C_{u,ECF,ss}$). As noted for quinidine in an *i.v.* infusion study, $C_{u,Br,ss}$ was roughly 3.5-fold lower than $C_{u,ECF,ss}$ [39]. In our case, $C_{u,Br,ss}$ was roughly 2-fold lower than $C_{u,ECF,ss}$ (Table V). In both studies, $C_{u,ECF,ss}$ would be considerably underestimated if this concentration was based on the unbound brain homogenate method (for $C_{u,Br,ss}$) instead of from microdialysis.

Additionally, the accuracy pertaining to BBB permeability obtained in a microdialysis study is dependent on the selection of a suitable probe compound. Quinidine appears to be suitable since it is a mildly lipophilic compound with a calculated clogD of 1.6 [39] and does not bind significantly to the microdialysis probe or tubing. It is metabolized by Cyp3a in liver, and though a well-characterized, specific P-gp substrate, there should be no influence of altered renal P-gp on the systemic clearance of quinidine. However, changes in brain P-gp upon 1,25$(OH)_2D_3$ treatment would alter the brain distribution of quinidine in the rat. Indeed, the brain to plasma concentration ratio differed by 36-fold between the *mdr1a/b* KO and WT mice [41]. However, data interpretation of VDR induction of MDR1 is that CYP3A induction is also observed within *in vitro* systems. In the Caco-2 cell system, treatment with 1,25$(OH)_2D_3$ up-regulated CYP3A4 protein and mRNA expression [11,42], and increased the metabolism of the CYP3A4 substrate, midazolam [42]. In human liver slices, CYP3A4 was increased upon exposure to 1,25$(OH)_2D_3$ [43]. However, in the rat liver where lower levels of Vdr protein exist [21], hepatic Cyp3a expression was unchanged with 1,25$(OH)_2D_3$ treatment, despite that higher intestinal Cyp3a1 and Cyp3a9 mRNA expression was found [21]. With these occurrences, we did not observe a significant change in plasma clearance between control and treated rats or in quinidine metabolism. The explanation of unchanged quinidine clearance in the face of unaltered liver Cyp3a but induced intestinal Cyp3a rests on the segregated flow patterns of the small intestine, with only a small flow perfusing the enterocyte region where most of the Cyp3a resides [44]. For intravenous administration, intestinal Cyp3a is unlikely to make a major contribution to metabolism of the drug [44]. It is also known that the expression and activity of Cyp3a in the brain is

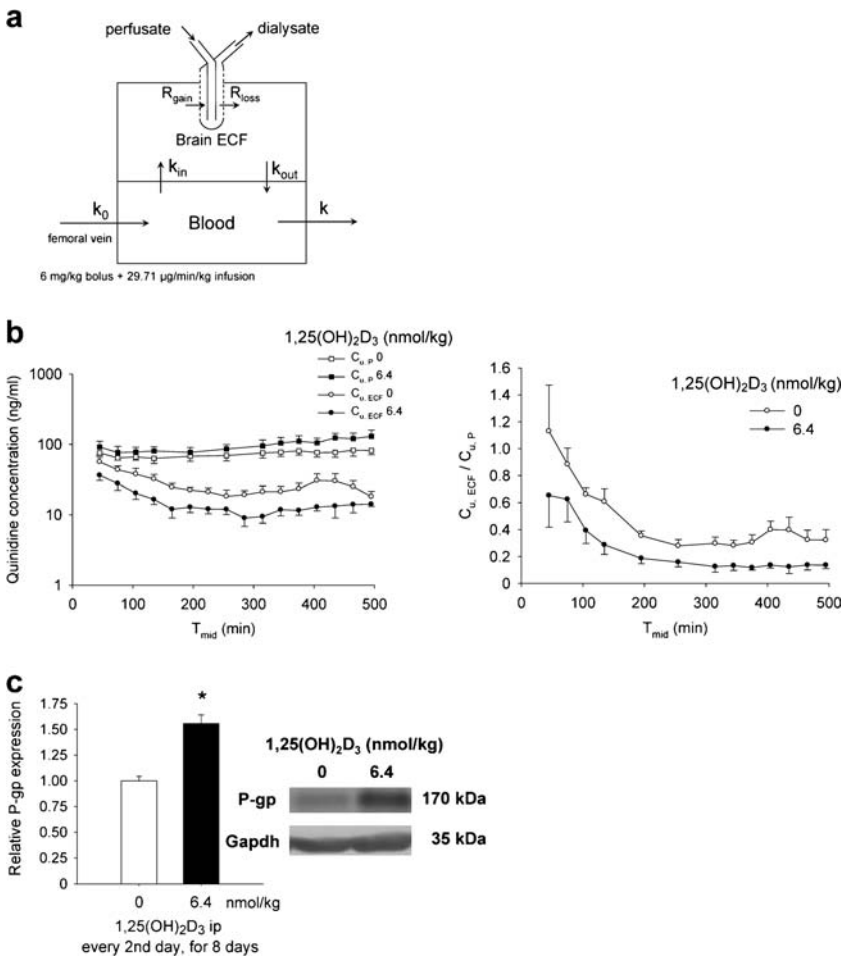

Fig. 4 The microdialysis setup (a) for comparing unbound plasma and brain ECF concentrations, and unbound brain ECF/unbound plasma concentration ratio (b), and P-gp levels (c) in the longitudinal study after treatment with vehicle, q2d × 4 then 6.4 nmol/kg $1,25(OH)_2D_3$ q2d × 4. $1,25(OH)_2D_3$ treatment lowered the unbound brain ECF concentration and the unbound brain ECF/unbound plasma concentration ratio at steady-state (b). Data are presented as mean ± S.E.M. "*" denotes $p < 0.05$ according to a paired Student's two-tailed *t* test. P-gp levels were induced in treated rats at the end of the microdialysis study, compared to matched, vehicle-treated controls (c). Data are presented as mean ± S.E.M. "*" denotes $p < 0.05$ according to Student's two-tailed *t* test.

substantially lower than that in hepatocytes [45], and it is unlikely that brain Cyp3a contributes to the cerebral metabolism of quinidine, as confirmed in the present study (data not shown). It is noted that $1,25(OH)_2D_3$ up-regulated Mdr1/P-gp in the kidney [46], an observation also verified in our study, which could increase tubular secretion and increase renal clearance of P-gp substrates. However, only 2% of quinidine is excreted unchanged into urine in rats [14], rendering any perturbations in this excretion pathway unimportant. Thus, quinidine plasma clearance is expected to remain unchanged whereas brain: plasma concentration ratio may be decreased.

Another factor that may influence quinidine plasma clearance and brain distribution is protein binding. The presence of indwelling catheters indeed altered the plasma protein binding of quinidine, as predicted by Terao and Shen [15], though there was no significant difference in binding post catheterization during the period when vehicle- and $1,25(OH)_2D_3$ microdialysis studies were carried out (day 12 *vs.* day 22). The $f_{u,P}$ in catheterized rats was lower, as was the blood:plasma concentration ratio of quinidine during repeated blood sampling, with the unbound fraction in blood being altered as a result of the decreased hematocrit (Tables III and IV). Since quinidine is rapidly cleared, the major determinant of clearance is hepatic blood flow and not protein binding, although changes in quinidine binding may change the distribution of quinidine in brain. Nevertheless, the investigation provided the correct $f_{u,P}$ in the estimation of $K_{ECF/P,uu}$ to assess brain distribution of quinidine. Upon appropriate correction for $f_{u,P}$, the $K_{ECF/P,uu}$ with $1,25(OH)_2D_3$ treatment (0.123 ± 0.0223) was lower than that of control (0.324 ± 0.0398) (Table V). Also, recovery values could affect the $K_{ECF/P,uu}$ results. A value of 0.173 for $K_{ECF/P,uu}$ has been reported [39], and the disparity to our control value (0.123) is likely due to differences in $f_{u,P}$ as well as different methods to determine recovery; ours was determined by *in vivo* retrodialysis and theirs, by the *in vitro* method. Recovery values determined *in vitro* are often poor predictors of *in vivo* recovery, as we have noted (0.591 ± 0.089 *vs.* 0.355 ± 0.028, compare Tables I and V). These findings highlight the importance of using rigorous controls when undertaking pharmacokinetic or microdialysis studies that utilize indwelling catheters.

In the current study, we demonstrated that treatment of rats with $1,25(OH)_2D_3$ activated rat cerebral Vdr and elevated Mdr1/P-gp expression at the BBB, which led to a lower

unbound ECF quinidine concentration and unbound ECF to plasma ratio at steady-state. Since $1,25(OH)_2D_3$ and other vitamin D analogs are commonly given to patients suffering from renal insufficiency [47], regulation of Mdr1/P-gp at the BBB by VDR has implications with respect to drug-drug interactions, because modulation of P-gp can exert a substantial effect on the distribution of drugs in the CNS [41]. In addition, $1,25(OH)_2D_3$ has recently been considered for concomitant therapy with other anticancer agents that are P-gp substrates [48]. Should these anticancer agents attempt to target the brain, sufficient therapeutic concentrations in the CNS may not be attained with $1,25(OH)_2D_3$ co-treatment. A thorough understanding of Mdr1/P-gp regulation by VDR at the BBB is important to prevent such interactions from occurring in the clinic.

ACKNOWLEDGMENTS AND DISCLOSURES

The authors have no conflict of interest to declare. This work was supported by the Canadian Institutes of Health Research (CIHR) and by NoAb BioDiscoveries (NoAb) and InterVivo Solutions (IVS). Matthew R. Durk was supported by a CIHR Strategic Training Grant in Biological Therapeutics and a Pfizer Canada Graduate Scholarship in Science and Technology. Additionally, we wish to thank employees of IVS, Sophie Pan and Julia Izhakova, for the bioanalysis of the microsomal, protein binding and blood; plasma ratio study samples and Victor Saldivia for carrying out the blood: plasma ratio studies. David K. H. Lee (NoAb and IVS) is thanked for approval of our collaborative efforts.

REFERENCES

1. Abbott NJ. Blood–brain barrier structure and function and the challenges for CNS drug delivery. J Inherit Metab Dis. 2013;36:437–49.
2. Lee G, Dallas S, Hong M, Bendayan R. Drug transporters in the central nervous system: brain barriers and brain parenchyma considerations. Pharmacol Rev. 2001;53:569–96.
3. Wang X, Sykes DB, Miller DS. Constitutive androstane receptor-mediated up-regulation of ATP-driven xenobiotic efflux transporters at the blood–brain barrier. Mol Pharmacol. 2010;78:376–83.
4. Bauer B, Hartz AM, Fricker G, Miller DS. Pregnane X receptor up-regulation of P-glycoprotein expression and transport function at the blood–brain barrier. Mol Pharmacol. 2004;66:413–9.
5. Narang VS, Fraga C, Kumar N, Shen J, Throm S, Stewart CF, *et al.* Dexamethasone increases expression and activity of multidrug resistance transporters at the rat blood–brain barrier. Am J Physiol Cell Physiol. 2008;295:C440–50.
6. Chow EC, Durk MR, Cummins CL, Pang KS. 1α,25-Dihydroxyvitamin D3 up-regulates P-glycoprotein via the vitamin D receptor and not farnesoid X receptor in both fxr(−/−) and fxr(+/+) mice and increased renal and brain efflux of digoxin in mice *in vivo*. J Pharmacol Exp Ther. 2011;337:846–59.
7. Durk MR, Chan GN, Campos CR, Peart JC, Chow EC, Lee E, *et al.* 1α,25-Dihydroxyvitamin D3-liganded vitamin D receptor increases expression and transport activity of P-glycoprotein in isolated rat brain capillaries and human and rat brain microvessel endothelial cells. J Neurochem. 2012;123:944–53.
8. Burris TP, Solt LA, Wang Y, Crumbley C, Banerjee S, Griffett K, *et al.* Nuclear receptors and their selective pharmacologic modulators. Pharmacol Rev. 2013;65:710–78.
9. Prufer K, Veenstra TD, Jirikowski GF, Kumar R. Distribution of 1, 25-dihydroxyvitamin D3 receptor immunoreactivity in the rat brain and spinal cord. J Chem Neuroanat. 1999;16:135–45.
10. Eyles DW, Smith S, Kinobe R, Hewison M, McGrath JJ. Distribution of the vitamin D receptor and 1 α-hydroxylase in human brain. J Chem Neuroanat. 2005;29:21–30.
11. Fan J, Liu S, Du Y, Morrison J, Shipman R, Pang KS. Up-regulation of transporters and enzymes by the vitamin D receptor ligands, 1α, 25-dihydroxyvitamin D3 and vitamin D analogs, in the Caco-2 cell monolayer. J Pharmacol Exp Ther. 2009;330:389–402.
12. de Lange EC, Danhof M, de Boer AG, Breimer DD. Critical factors of intracerebral microdialysis as a technique to determine the pharmacokinetics of drugs in rat brain. Brain Res. 1994;666:1–8.
13. Martignoni M, Groothuis G, de Kanter R. Comparison of mouse and rat cytochrome P450-mediated metabolism in liver and intestine. Drug Metab Dispos. 2006;34:1047–54.
14. Fremstad D, Jacobsen S, Lunde KM. Influence of serum protein binding on the pharmacokinetics of quinidine in normal and anuric rats. Acta Pharmacol Toxicol (Copenh). 1977;41:161–76.
15. Teraoand N, Shen DD. Alterations in serum protein binding and pharmacokinetics of l-propranolol in the rat elicited by the presence of an indwelling venous catheter. J Pharmacol Exp Ther. 1983;227:369–75.
16. Liu L, Mak E, Tirona RG, Tan E, Novikoff PM, Wang P, *et al.* Vascular binding, blood flow, transporter, and enzyme interactions on the processing of digoxin in rat liver. J Pharmacol Exp Ther. 2005;315:433–48.
17. de Lange EC, Danhof M, de Boer AG, Breimer DD. Methodological considerations of intracerebral microdialysis in pharmacokinetic studies on drug transport across the blood–brain barrier. Brain Res Brain Res Rev. 1997;25:27–49.
18. Chan GN, Saldivia V, Yang Y, Pang H, de Lannoy I, Bendayan R. *In vivo* induction of P-glycoprotein expression at the mouse blood–brain barrier: an intracerebral microdialysis study. J Neurochem. 2013;127:342–52.
19. Lowry OH, Rosebrough NJ, Farr AL, Randall RJ. Protein measurement with the Folin phenol reagent. J Biol Chem. 1951;193:265–75.
20. Jonesand G, Tenenhouse HS. 1,25(OH)2D, the preferred substrate for CYP24. J Bone Miner Res. 2002;17:179–81.
21. Chow EC, Maeng HJ, Liu S, Khan AA, Groothuis GM, Pang KS. 1α,25-Dihydroxyvitamin D3 triggered vitamin D receptor and farnesoid X receptor-like effects in rat intestine and liver *in vivo*. Biopharm Drug Dispos. 2009;30:457–75.
22. Sugihara N, Furuno K, Kita N, Murakami T, Yata N. Distribution of quinidine in rats with carbon tetrachloride-intoxicated hepatic disease. J Pharmacobiodyn. 1992;15:167–74.
23. Pollack GM, Brouwer KL, Demby KB, Jones JA. Determination of hepatic blood flow in the rat using sequential infusions of indocyanine green or galactose. Drug Metab Dispos. 1990;18:197–202.
24. Sato Y, Asoh T, Oizumi K. High prevalence of vitamin D deficiency and reduced bone mass in elderly women with Alzheimer's disease. Bone. 1998;23:555–7.
25. Wilkins CH, Sheline YI, Roe CM, Birge SJ, Morris JC. Vitamin D deficiency is associated with low mood and worse cognitive performance in older adults. Am J Geriatr Psychiatry. 2006;14:1032–40.
26. Evatt ML, Delong MR, Khazai N, Rosen A, Triche S, Tangpricha V. Prevalence of vitamin d insufficiency in patients with Parkinson disease and Alzheimer disease. Arch Neurol. 2008;65:1348–52.

27. Hollo A, Clemens Z, Kamondi A, Lakatos P, Szucs A. Correction of vitamin D deficiency improves seizure control in epilepsy: a pilot study. Epilepsy Behav. 2012;24:131–3.
28. Kalueff AV, Minasyan A, Keisala T, Kuuslahti M, Miettinen S, Tuohimaa P. Increased severity of chemically induced seizures in mice with partially deleted Vitamin D receptor gene. Neurosci Lett. 2006;394:69–73.
29. Brown J, Bianco JI, McGrath JJ, Eyles DW. 1,25-Dihydroxyvitamin D3 induces nerve growth factor, promotes neurite outgrowth and inhibits mitosis in embryonic rat hippocampal neurons. Neurosci Lett. 2003;343:139–43.
30. Orme RP, Bhangal MS, Fricker RA. Calcitriol imparts neuroprotection *in vitro* to midbrain dopaminergic neurons by upregulating GDNF expression. PLoS ONE. 2013;8:e62040.
31. Brewer LD, Thibault V, Chen KC, Langub MC, Landfield PW, Porter NM. Vitamin D hormone confers neuroprotection in parallel with downregulation of L-type calcium channel expression in hippocampal neurons. J Neurosci. 2001;21:98–108.
32. Zanatta L, Goulart PB, Goncalves R, Pierozan P, Winkelmann-Duarte EC, Woehl VM, *et al.* 1alpha,25-dihydroxyvitamin D(3) mechanism of action: modulation of L-type calcium channels leading to calcium uptake and intermediate filament phosphorylation in cerebral cortex of young rats. Biochim Biophys Acta. 2012;1823:1708–19.
33. Kim RB. Drugs as P-glycoprotein substrates, inhibitors, and inducers. Drug Metab Rev. 2002;34:47–54.
34. Lam FC, Liu R, Lu P, Shapiro AB, Renoir JM, Sharom FJ, *et al.* β-Amyloid efflux mediated by p-glycoprotein. J Neurochem. 2001;76:1121–28.
35. Hammarlund-Udenaes M. Active-site concentrations of chemicals - are they a better predictor of effect than plasma/organ/tissue concentrations? Basic Clin Pharmacol Toxicol. 2010;106:215–20.
36. Shuaib A, Xu K, Crain B, Siren AL, Feuerstein G, Hallenbeck J, *et al.* Assessment of damage from implantation of microdialysis probes in the rat hippocampus with silver degeneration staining. Neurosci Lett. 1990;112:149–54.
37. de Lange EC, Danhof M, Zurcher C, de Boer AG, Breimer DD. Repeated microdialysis perfusions: periprobe tissue reactions and BBB permeability. Brain Res. 1995;702:261–5.
38. de Lange EC, de Bock G, Schinkel AH, de Boer AG, Breimer DD. BBB transport and P-glycoprotein functionality using MDR1A (−/−) and wild-type mice. Total brain *versus* microdialysis concentration profiles of rhodamine-123. Pharm Res. 1998;15:1657–65.
39. Liu X, Van Natta K, Yeo H, Vilenski O, Weller PE, Worboys PD, *et al.* Unbound drug concentration in brain homogenate and cerebral spinal fluid at steady state as a surrogate for unbound concentration in brain interstitial fluid. Drug Metab Dispos. 2009;37:787–93.
40. Syvanen S, Schenke M, van den Berg DJ, Voskuyl RA, de Lange EC. Alteration in P-glycoprotein functionality affects intrabrain distribution of quinidine more than brain entry-a study in rats subjected to status epilepticus by kainate. AAPS J. 2012;14:87–96.
41. Doran A, Obach RS, Smith BJ, Hosea NA, Becker S, Callegari E, *et al.* The impact of P-glycoprotein on the disposition of drugs targeted for indications of the central nervous system: evaluation using the MDR1A/1B knockout mouse model. Drug Metab Dispos. 2005;33:165–74.
42. Schmiedlin-Ren P, Thummel KE, Fisher JM, Paine MF, Lown KS, Watkins PB. Expression of enzymatically active CYP3A4 by Caco-2 cells grown on extracellular matrix-coated permeable supports in the presence of 1α,25-dihydroxy vitamin D3. Mol Pharmacol. 1997;51:741–54.
43. Khan AA, Chow EC, van Loenen-Weemaes AM, Porte RJ, Pang KS, Groothuis GM. Comparison of effects of VDR *versus* PXR, FXR and GR ligands on the regulation of CYP3A isozymes in rat and human intestine and liver. Eur J Pharm Sci. 2009;37:115–25.
44. Cong D, Doherty M, Pang KS. A new physiologically based, segregated-flow model to explain route-dependent intestinal metabolism. Drug Metab Dispos. 2000;28:224–35.
45. Woodland C, Huang TT, Gryz E, Bendayan R, Fawcett JP. Expression, activity and regulation of CYP3A in human and rodent brain. Drug Metab Rev. 2008;40:149–68.
46. Chow EC, Sun H, Khan AA, Groothuis GM, Pang KS. Effects of 1α, 25-dihydroxyvitamin D3 on transporters and enzymes of the rat intestine and kidney *in vivo*. Biopharm Drug Dispos. 2010;31:91–108.
47. M. Rodriguez, J.R. Munoz-Castaneda, Y. Almaden. Therapeutic Use Of Calcitriol. Curr Vasc Pharmacol (2013).
48. Muindi JR, Peng Y, Potter DM, Hershberger PA, Tauch JS, Capozzoli MJ, *et al.* Pharmacokinetics of high-dose oral calcitriol: results from a phase 1 trial of calcitriol and paclitaxel. Clin Pharmacol Ther. 2002;72:648–59.